



UNIVERSITY OF INDONESIA

**ROOM TEMPERATURE CHARACTERISATION OF AZ31
MAGNESIUM ALLOY PLATE**

FINAL PROJECT

HARYMAN LAMHOT MANULLANG

0404840018

**S-1 INTERNATIONAL PROGRAM
ENGINEERING FACULTY
DEPARTMENT OF METALLURGY AND MATERIALS
DEPOK
DESEMBER 2008**



UNIVERSITY OF INDONESIA

**ROOM TEMPERATURE CHARACTERISATION OF AZ31
MAGNESIUM ALLOY PLATE**

FINAL PROJECT

This Final project report is prerequisite to obtain Sarjana Teknik

HARYMAN LAMHOT MANULLANG

0404840018

S-1 INTERNATIONAL PROGRAM

ENGINEERING FACULTY

DEPARTMENT METALLURGY AND MATERIALS

DEPOK

DESEMBER 2008

AUTHENTICATION PAGE

I state that this project proposal with the title below:

ROOM TEMPERATURE CHARACTERISATION OF AZ31 MAGNESIUM ALLOY PLATE

As far as I concern is not duplication from other project proposal which are published or has been used to obtain a degree in University of Indonesia, except some part which are referenced.

Name : Haryman Lamhot Manullang

NPM : 0404840018

Signature :

DD/MM/YY : 6 January 2009

VALIDATION PAGE

This Final project report is proposed by:

Name : Haryman Lamhot Manullang
NPM : 0404840018
Course Program : Metallurgy and Material Engineering
Project Title : Room Temperature Characterisation of AZ31
Magnesium Alloy Plate

Produce in order to fulfill the requirement to become Sarjana Teknik in the Department of Material Engineering, Faculty of Engineering University of Indonesia. This project report has been examined and approved on the project presentation.

Depok, Desember 2008

Supervisor,

Dr.Ir. Bondan Tiara Sofyan, M.Si

NIP. 131 992 220

PREFACE

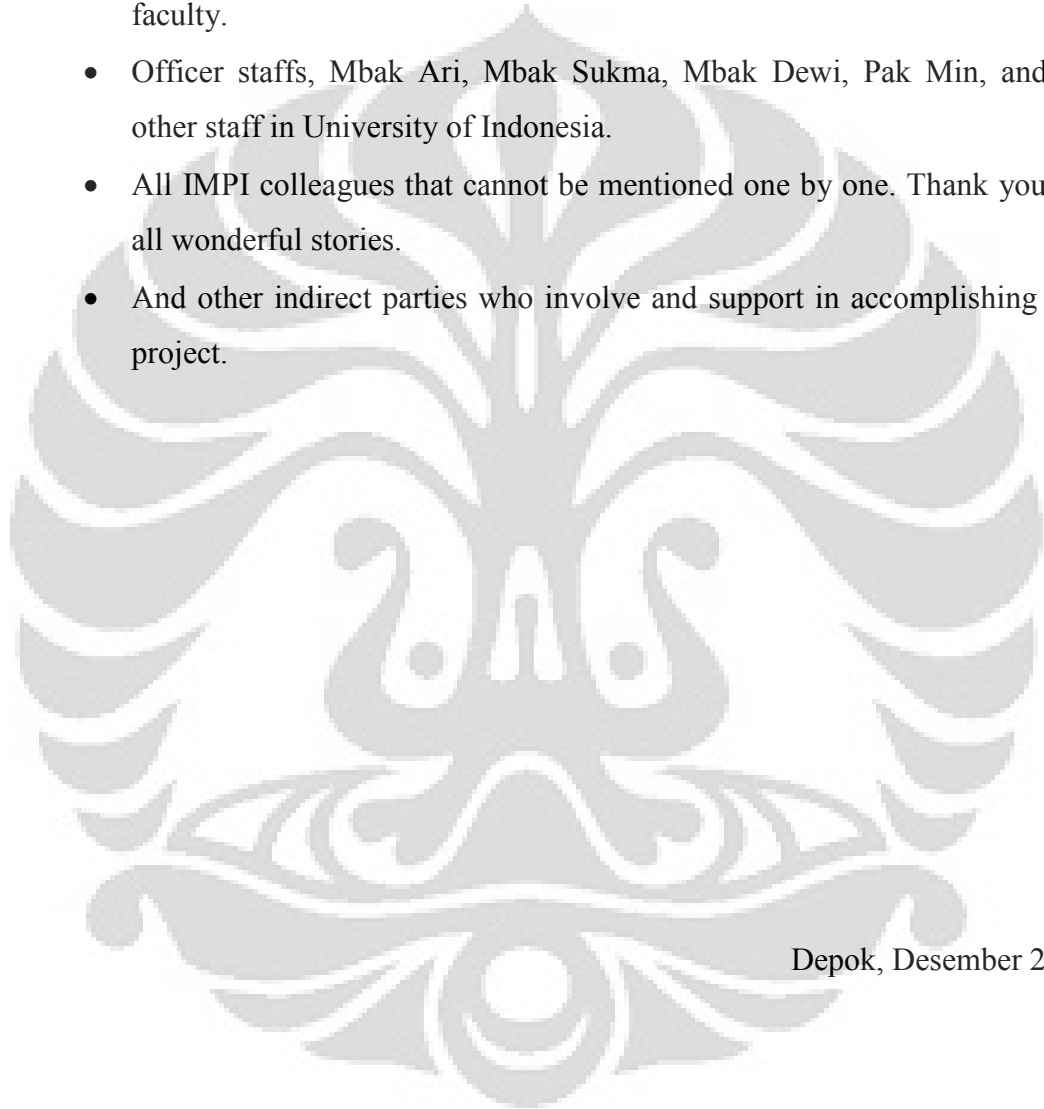
The research with the title of “ROOM TEMPERATURE CHARACTERISATION OF AZ31 MAGNESIUM ALLOY PLATE” is accomplished as an academic requirement to obtain Bachelor of Engineering in Monash University and Sarjana Teknik in University of Indonesia.

The writer is aware that this research is still far from excellence and has many limitations, so it might be needed further improvement and deeper investigations.

The writer wants to convey his gratitude to all parties that have helped the writer finishing this research. Many thanks to:

- God Almighty, for giving the strength, wisdom and conviction to finish this research.
- My supervisor in Monash University, A/Professor Chris Davies for all his direction, advice, patient and support throughout my study in Monash University.
- My supervisor in University of Indonesia, Dr.Ir. Bondan Tiara Sofyan, M.Si for all her guidance, advice, patient and especially support in this past 4 years of my study both in University of Indonesia and Monash University.
- My beloved family and parents, for always praying and giving both financial and spiritual support to accomplished this degree. My older sister and her husband for cheering me up during the final examination.
- Mr. Graham Prior, Mrs. Jeanette, Mr. Silvio Mantievichi and Mr. Irek Kozinski for providing me all laboratories tools, assisting in using the apparatus, and also time to share thoughts and ideas for this project.
- My lovely friends in international class, Dhiani Satiti, Leo Gading Mas, Rachmat Imansyah, Andika Ibrahim, Diko Yudazaki and Rahardian Ghazali together with all IMPI Brisbane.

- All Materials Engineering student in Monash University, Matthew Zona, Thero Therence Tutu, Ghwala Mooketsi, Steven Hughes, Taeil Noh, Ling Qiu, Thai Nguyen, Stuart Moffit, Sky Loo, and all other Monash students.
- All Metalurgy and Material student 2004 in University of Indonesia, Martino Hutasoit, Kaspar Purba, Sandy Sipayung, Vita Astini, Benny Muchtar, Maro Pane and all other engineering student in engineering faculty.
- Officer staffs, Mbak Ari, Mbak Sukma, Mbak Dewi, Pak Min, and all other staff in University of Indonesia.
- All IMPI colleagues that cannot be mentioned one by one. Thank you for all wonderful stories.
- And other indirect parties who involve and support in accomplishing this project.



Depok, Desember 2008

Haryman Lamhot Manullang

**HALAMAN PERNYATAAN PERSETUJUAN PUBLIKASI
TUGAS AKHIR UNTUK KEPENTINGAN AKADEMIS**

Sebagai sivitas akademik Universitas Indonesia, saya yang bertanda tangan di bawah ini:

Nama : Haryman Lamhot Manullang
NPM : 0404840018
Program studi : S-1 Program Internasional
Departemen : Teknik Metalurgi dan Material
Fakultas : Teknik
Jenis Karya : Skripsi

Demi pengembangan ilmu pengetahuan, menyetujui untuk memberikan kepada Universitas Indonesia **Hak Bebas Royalti Noneksklusif (Non-exclusive Royalty-Free Rights)** atas karya ilmiah saya yang berjudul:

**ROOM TEMPERATURE CHARACTERISATION OF AZ31
MAGNESIUM ALLOY PLATE**

Beserta perangkat yang ada (jika diperlukan). Dengan Hak Bebas Royalti Noneksklusif ini Universitas Indonesia berhak menyimpan, mengalihmedia/format-kan, mengelola dalam bentuk pangkalan data (database), merawat, dan mempublikasikan tugas akhir saya tanpa meminta izin dari saya selama tetap mencantumkan nama saya sebagai penulis/pencipta dan pemilik Hak Cipta.

Demikian pernyataan ini saya buat dengan sebenarnya.

Dibuat di : Depok

Pada tanggal : 6 Januari 2009

Yang menyatakan

(Haryman L. Manullang)

ABSTRACT

Name : Haryman Lamhot Manullang

Study program: Metallurgy and Material Engineering

Title : ROOM TEMPERATURE CHARACTERISATION OF AZ31
MAGNESIUM ALLOY PLATE

Recently, advanced technologies have put much attention on the materials selection as an alternative way to reduce the weight of material. Taking into account electronic devices, automobiles, aeronautics, and structural applications they are all required immense raw product. Magnesium and its alloys as one of the lightest metal ($\rho = 1.8 \text{ g/m}^3$) has attracted much intentions for an alternative metal alloy. Such good properties owned in magnesium including good castability, good machinability as well weldability and considerably cheap have made more convenient way for magnesium alloys to be used. However, its poor formability at room temperature is the major drawback of this material.

Therefore, this project is intended to investigate the properties of AZ31 magnesium alloy especially for uniaxial tensile test at relatively low strain rate. Tensile properties were observed on the yield strength and elastic modulus which seems the crucial factor for magnesium tested at relatively low temperature. Slight dependency of plate orientations to the tensile properties for plate samples and tensile directions for sheet samples with three different sample thicknesses were also carried out. The experiment was done with the use of non-contact extensometer of Mini Instron Tensile Test.

The main conclusion from the present study is that the thickness and the samples orientations affected tensile direction properties of the sheet samples. Microyielding occurred during the test which resulted in declining of modulus as the thickness increases. By contrast ultimate tensile strength, yield strength and ductility are generally increased as the thickness increased.

Key words:

Magnesium alloys, tensile test, sample orientations

TABLE OF CONTENTS

TITLE PAGE	i
VALIDATION PAGE	ii
AUTHENTICATION PAGE	iii
PREFACE.....	iv
PUBLICATION AGREEMENT FORM	vi
ABSTRACT	vii
TABLE OF CONTENTS.....	viii
LIST OF FIGURES	x
LIST OF TABLES	xi
APPENDIX	xii
CHAPTER I INTRODUCTION.....	1
1.1. Background.....	1
1.2. Objectives	2
1.3. Scope of Research	2
CHAPTER II LITERATURE REVIEW.....	3
2.1. Magnesium Alloy	3
2.1.1 Basic Properties	3
2.1.2 Crystal Structure	4
2.2. Deformation in Magnesium Alloy.....	5
CHAPTER III EXPERIMENTAL METHODS	7
3.1. Flowchart of Project.....	7
3.2. Materials and Equipment	8
3.2.1. Materials	8
3.2.2. Equipment	8
3.3. Testing and Observation	9
3.3.1. Cutting	9
3.3.1.1. Plate Orientation	9
3.3.1.2. Thickness	9
3.3.2. Metallography	9
3.4. Tensile Test	11

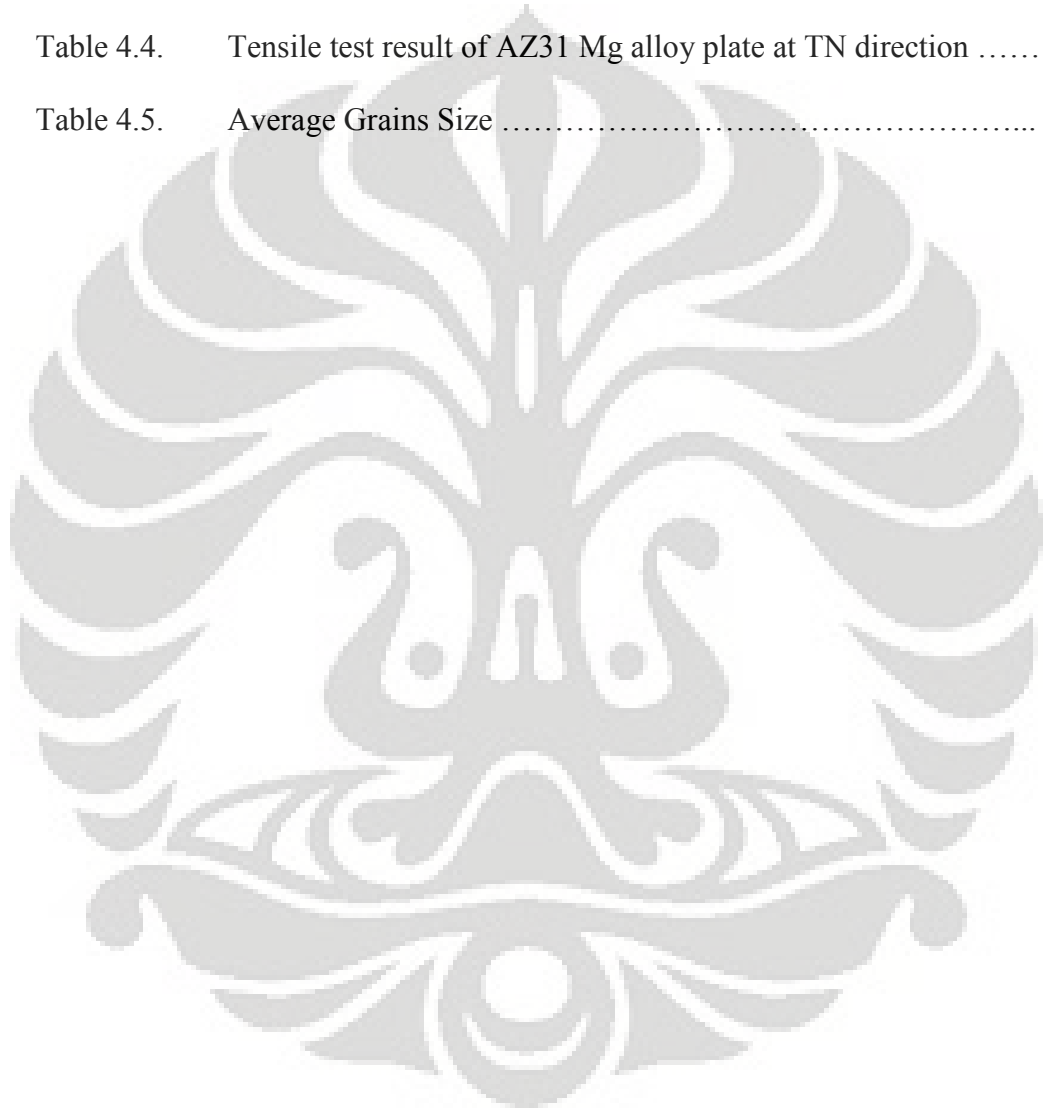
CHAPTER IV RESULTS AND DISCUSSION	14
4.1. Tensile Characteristics of AZ31 Magnesium Alloy Plate	14
4.1.1. Elastic Modulus	16
4.1.2. Ultimate Tensile Strength	17
4.1.3. 0.2% Proof Strength	17
4.1.4. Elongation-to-failure (EL)	19
4.1.5. Strain rate sensitivity	21
4.2. Microscopic Observation	22
4.2.1. Optical Micrograph	23
4.3.1.1. As-received	23
4.3.1.2. As-deformed	24
4.3. Macroscopic Images	27
CHAPTER V CONCLUSION AND FUTURE WORK	29
REFERENCES	31
APPENDIX	32

LIST OF FIGURES

Figure 2.1.	Schematic Diagram	4
	(a) Slab casting process	4
	(b) Direct extrusion process	4
Figure 2.2.	Slip planes in hcp material	4
Figure 3.1.	Plate orientation diagram	8
Figure 3.2.	Illustration of specimen sectioning	9
Figure 3.3.	Schematic diagram of tensile specimen	11
Figure 3.4.	True Strain Vs Strain Rate	12
Figure 3.5.	Model of MiniInstron 5848	13
Figure 4.1.	Graph of Elastic modulus	17
Figure 4.2.	Graph of Ultimate Tensile Strength	18
Figure 4.3.	Graph of Yield Strength	19
Figure 4.4.	Graph of Total Elongation	20
Figure 4.5.	Graph of Strain rate sensitivity	21
Figure 4.6.	Microstructure of as-received specimen	24
Figure 4.7.	Microstructure of as-deformed specimen	25
Figure 4.8.	Macroscopic features of failure specimen	28

LIST OF TABLES

Table 4.1.	Tensile test result of AZ31 Mg alloy plate at RT direction	15
Table 4.2.	Tensile test result of AZ31 Mg alloy plate at TR direction	15
Table 4.3.	Tensile test result of AZ31 Mg alloy plate at NR direction	15
Table 4.4.	Tensile test result of AZ31 Mg alloy plate at TN direction	15
Table 4.5.	Average Grains Size	23



CHAPTER I

INTRODUCTION

1.1. BACKGROUND

The competition of light metal alloys in immense technological applications has encouraged metal industries to intensively explore more about the light-weight structural metal especially magnesium alloys. Due to its superior strength-to-weight ratio with density of one-third dense than aluminum, excellent castability and recyclability have made magnesium alloys as an alternative metal for further technical applications such as aeronautics, electronics, and housing utensils [1]. Because of that, some manufacturers have already changed the production of component such as cylinder-head covers, gear housings, dashboard frames from aluminum or steel to magnesium. Most components are die-cast, since this process takes most advantage of magnesium's good castability. Parts made by other production methods are used very rarely in automobiles including wrought product.

Magnesium alloy AZ31 is commercially known as wrought product which produced from extrusion process. The main problem encountered with magnesium cast products is mainly comes from its poor formability which is hard to bend at room temperature. In industrial point of view, materials with large extent of ductility would be very useful in substantially lowering the cost and could be utilized for much wider applications, such as automobile parts. However, this case would never been achieved for Magnesium product unless such a microalloying element been added along with the refined grains structure. There has been lot of article investigating the behavior of magnesium at elevated temperature together with the explanation of deformation modes. To this end, formability of magnesium alloys at room temperature becomes much more interest issue rather than focusing on changes in the forming process to achieve better properties.

Therefore, this project studied the room temperature characterization of AZ31 magnesium alloy plate. Effects of sample thickness and plate orientation were analyzed through tensile testing and metallographic observation.

1.2. OBJECTIVES

The objectives of this present study are:

- To investigate the room temperature tensile properties of AZ31 magnesium alloy plate.
- To investigate the effect of sample thickness on the tensile properties and microstructure of AZ31 magnesium alloy plate.
- To investigate the effect of sample direction on the tensile properties and microstructure of AZ31 magnesium alloy plate.
- To study the possible mechanism of room temperature deformation of AZ31 magnesium alloy plate.

1.3. SCOPE OF RESEARCH

The present study used plate samples with thickness of 0.2, 0.5 and 1 mm and observed tensile properties at four different direction: NR, RT, TD, and TN. Conventional tensile testing and jump testing were conducted by using Non-Contact Extensometer (NCX[®]) Mini Instron Tensile Test Machine, while microstructure was observed by using optical microscope. Quantitative metallography was also performed by using planimetry method.

CHAPTER II

LITERATURE REVIEW

2.1 MAGNESIUM ALLOY

2.1.1. Basic Properties

In general, metal processing of magnesium is similar with other metal processes. The molten magnesium is formed through casting process. The continuation of the casting is then known as extrusion. This post-treatment of metal processing is different to certain extent in which the final geometry has been determined. In the case of magnesium alloys AZ31, the product produced from extrusion. The common products of AZ31 are largely used as automotive body parts and electronic devices frames.

The production of magnesium is temperature sensitive by which oxidation is easily formed during the heat treatment. Therefore, such a cautious treatment had to be done when dealing in hot temperature process. It is found at high temperature ($T > \sim 0.6T_m$) the mechanical properties of magnesium significantly improved in terms of ductility [2,3]. Such a deeper investigation on the plasticity behaviour of magnesium has been studied from the mid of 1960s. The study have investigated the extensive application of slip trace analyses and constrained deformation experiment whom concluded that among three different slip systems in single crystal Mg only basal plane $\langle c \rangle$ consume less energy for plastic deformation to be occurred [4]. According to reported data, the critical resolved shear stress (CRSS) of basal slip system at room temperature is approximately 1/100 those of non-basal slip systems on prismatic $\langle a \rangle$ and pyramidal planes $\langle c+a \rangle$ [5]. Further to this reported data, texture plays important role in deformation history and deformation mechanism. To this end, there remain some uncertainties about which deformation modes are responsible for developing a given texture type, and which texture promote a given deformation mode. Therefore, the deformation behavior of magnesium strip in the low strain region prior to the yield point and strain rate changes in a standard tensile test appears to be an important factor in determining formability

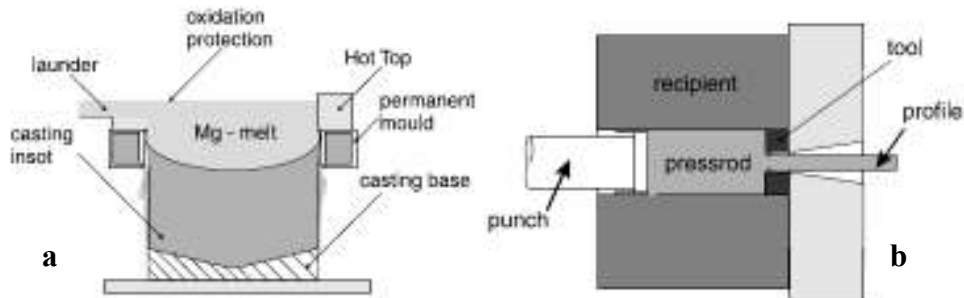


Figure 2.1. Schematic diagram of (a) Slab-casting process, (b) Direct extrusion process [6].

The basic casting process of magnesium is shown in **Fig. 2.1(a)** while the extruded product is shown in **Fig. 2.1(b)**. Deformation at room temperature is the primary challenge for magnesium. However, with relatively adequate amount of alloying elements the major problem can be solved. Also with decent and accurate geometry tools, deformation can be done easily.

2.1.2. Crystal Structure

Pure magnesium materials possess hexagonal close-packed (hcp) crystal structure. This hexagonal unit cell has four axes inside the unit cell which well-known as lattice parameter. In terms of axial relationships, hexagonal unit cell has lattice parameter $a = b \neq c$ followed by interaxial angles $\alpha = \beta = 90^\circ$, $\gamma = 120^\circ$. Concomitantly, steel and aluminum which has FCC crystal structure have symmetric lattice parameter. It is only need one slip system in order the plastic deformation takes place for FCC material whilst HCP structure one needs more than one deformation systems with very complex lattice parameter. A deeper interpenetration about the hexagonal unit cell is shown in **Fig. 2.2**.

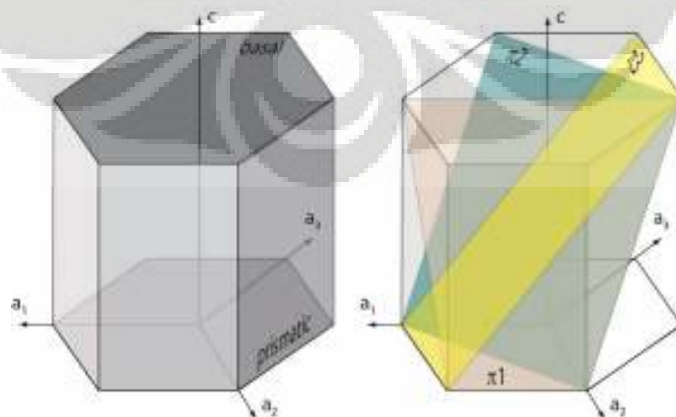


Figure 2.2 Slip planes in hcp material: basal and prismatic planes (left), pyramidal (π_1 : {01-11}, π_2 : {1-22}, π_3 : {10-12} planes) (right). [7]

Barnett stated that the change in proof (yield) stress of AZ31 sheet in tension as a function of temperature and strain rate has been studied since at least 1950s and data relating to the phenomenon appear in a number of magnesium design handbooks [3]. At this era, the technology is limited for further investigation, for example to which deformation modes might be accommodated based on textures measurement (EBSD). To this end, just by in the early 1970s Stohr and Poirier have investigated non-basal dislocations of pyramidal plane $\langle c+a \rangle$ confirmed to be active within magnesium [3]. At this stage, which the dislocation slips have to responsible for the deformation modes is only applied at high homologous temperatures.

Strength of Magnesium alloys is very sensitive to grain size as can be seen from the value of k in the Hall-Petch relationship: $\sigma = \sigma_0 + kd^{-0.5}$. For magnesium alloys, $k=210 \text{ MPa}\cdot\text{mm}^{1/2}$ which is thrice the value for aluminium alloys ($k=70 \text{ MPa}\cdot\text{mm}^{1/2}$) [8]. The ductility of magnesium is strongly related with the forming limit diagram (FLD) properties. It is the ability of material to be formed normally under deep-drawing process.

2.2 DEFORMATION IN MAGNESIUM ALLOY

In magnesium there are two dominant deformation mechanism, crystallographic slip and mechanical twin [6]. In terms of slip systems, a basic requirement of plastic deformation has to be fulfilled that is 5 independent deformation systems of the classical von Mises criterion. Since basal slip provides only two independent systems, the activation of non-basal slips and/or twinning is in significant importance for improving mechanical properties. As above-mentioned, the activation of non-basal systems is strongly influenced by the texture developed after any thermo-mechanical process, and it is directly related to the mechanical anisotropy [1]. Another two of non-basal plane still have less than 5 independent slip systems. With reference to the Taylor criterion, it is noted that prismatic slip $\langle c+a \rangle$ would offer two independent slip modes while pyramidal slip would offer four independent slip modes [2]. To this end, there has

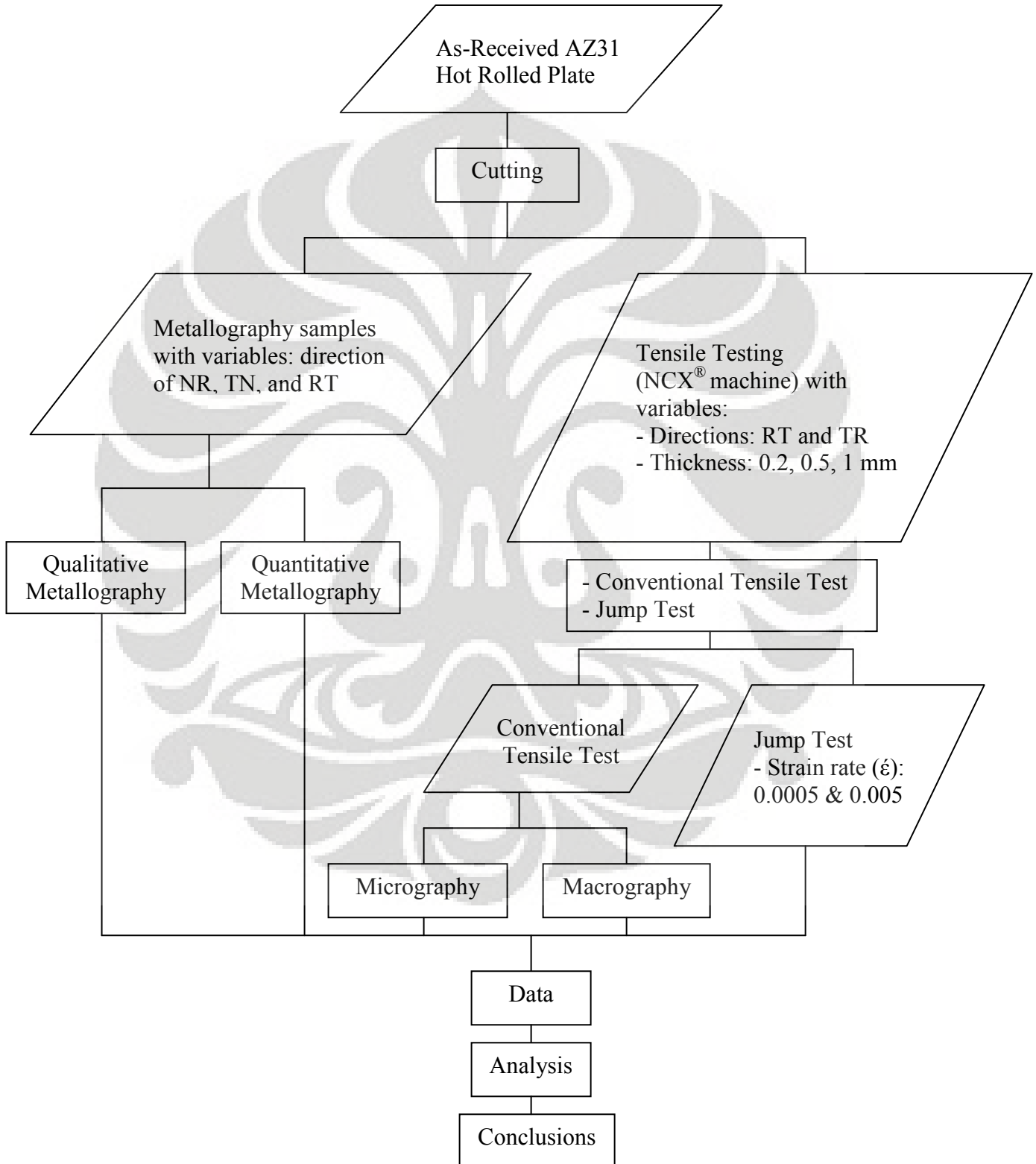
been some literature review discussed on the dependency of the activated deformation modes on the texture evolution in Magnesium alloys and vice versa.

Apart from dislocation slip, another important aspect on magnesium is strong propensity for mechanical twinning especially the $\{10\bar{1}2\}$ $\langle 10\bar{1}1 \rangle$ tension twin [2]. This tension twin forms a triangular plane across the interior of single hexagonal crystal structure. Therefore, it is well established that twinning is a polar mechanism. However, the amount strain that twinning can accommodate is directly proportional to the volume fraction of crystal which has twinned. This also influenced from the chemical composition of the alloying elements. *Agnew and Duygulu* investigated from previous study and found for the primary twinning mode observed to operate within magnesium $\{10\bar{1}2\}$, the twinning shear is only 0.13 and thus, the maximum tensile strain that twinning may accommodate is about 0.065 or 6.5% true strain [2]. Barely keeping this idea in mind because in the experimental project; indeed, the magnesium samples have such a voice at that ranges of strain. In latter case, people called it “twinning crying”.

There have been almost 70 years the related issue in magnesium metal being studied. However, the mystery of poor workability of magnesium at room temperature is still much interest to this end. One of the explanations is due to large anisotropy produced within this hexagonal metal (HM). It has found material with high c/a ratio can be classified as kinking nonlinear elastic (KNE) [9]. Further to this, deformation of solids materials at very low strains $<1\%$ have indicated the occurrence of kinking bands (KBs). These kinking bands are strongly related with microstructure by which in fine grain (FG) samples, microyielding is taken in the activation of primary slip (basal). The summary of these incipient kinking bands (IKBs) are nature's solution to plastic anisotropy deformation particularly hexagonal metals which have high c/a ratio and considerably fine grain structure were subjected to experience damping and microyielding phenomenon and significantly affect the tensile behaviour especially in linear elastic region [9].

CHAPTER III
EXPERIMENTAL METHODS

3.1. FLOWCHART OF PROJECT



3.2. MATERIALS AND EQUIPMENT

3.2.1. Materials

- AZ31 magnesium alloy plate
- SiC paper
- Polisher clothing
- M2 Picric Acid Etchant
- Al₂O₃ liquid suspension

3.2.2. Equipment

- Buehler slow speed cutting saw
- Struers grinding machine
- Saphir 320 polishing machine
- Olympus optical micrograph
- Mini Instron 5848 Tensile Test with integrated video camera
- LED lights
- Sony Camera Digital 7.2 MP
- Marking template

3.3. TESTING AND OBSERVATION

3.3.1. Cutting

The initial AZ31 magnesium alloy is a hot rolled plate. In order to test the sample with Mini Instron Tensile Test, there are four variables of plate orientation RT, TR, NR, and TN. **Fig. 3.1** shows the two variables RT and TR which also known as longitudinal and transverse direction while the other two variables NR and TN are shown in **Fig. 3.2**.

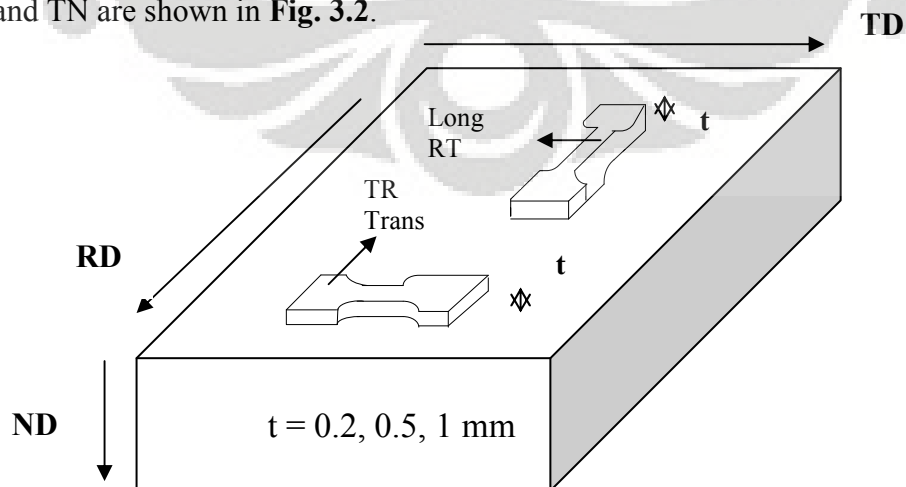


Figure 3.1. Plate Orientation diagram of RT and TR orientation

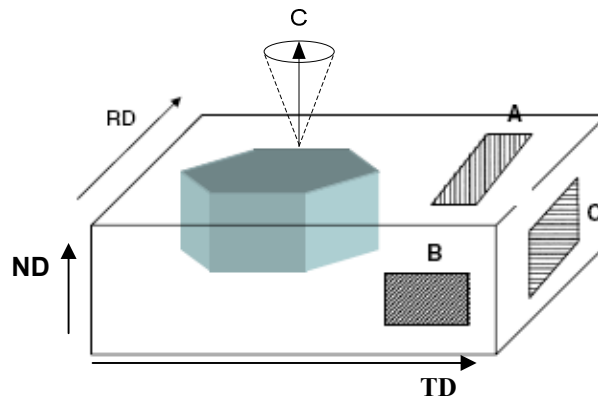


Figure 3.2 Schematic illustrations of specimen sectioning with c-axis lies relative to tensile axis, (a) basal specimen (RT), (b) off-basal specimen (NR), (c) off-basal specimen (TN).

3.3.1.1. Plate Orientation

The two letter code identification of plate orientation is based on the axis of tensile direction. The RT specimen, for example, describes the direction of uniaxial tensile test is parallel to the rolling direction (RD) and perpendicular with transverse direction (TD). As it shown in **Fig. 3.1** the specimens were taken in two directions along and across the rolling direction which then corresponds to longitudinal (RT) and transverse (TR) direction. **Fig. 3.2** shown the specimen sectioning corresponds to the basal and off-basal plane. For example, in A sectioning the c-axis is perpendicular to the plate. The other two specimen sectioning NR and TN belong to off-basal plane.

3.3.1.2. Thickness

Initially, the thickness variables were obtained by cutting machine instead of rolling process to produce 0.2, 0.5, and 1 mm thickness. Some of the specimens have the actual thickness different with the nominal thickness which then found to have ± 0.05 mm deviation. All specimens were cut according to ASTM E8M for standard of tensile sample.

3.3.2. Metallography

The metallography method was conducted before and after tensile test. The microstructure investigation before tensile test was prepared by cutting the AZ31 magnesium alloy from a big chunk of hot-rolled plate. The use of Buehler slow speed saw was very necessary for cutting magnesium alloy sample into three different face orientations that are RT, TN and NR. The details of the plate orientation can be seen in **Fig. 3.1** and **Fig. 3.2**.

The metallography after tensile test were conducted based on each sample variable for tensile test. The directions of the images for both before and after tensile test were taken through the thickness direction near to the fracture region. General metallography preparation steps have been conducted according to several procedures of grinding, polishing and etching.

- Grinding and Polishing

There are four subsequent SiC papers that have been used grit sizes starting from 400, 800, 1200, and 3200. It was followed by manual polishing of the sample surface. Two different types of polishing cloths were used with Al₂O₃ liquid suspension. This is aimed for eliminating defect and coarse scratch from previous grinding process.

- Etching

Once the grinding and polishing have been completed, the samples were then ready to be observed under optical microscope. In order to reveal the grains structure, a chemical solution labeled with M2 magnesium etchant was used. It consists of 12 gram picric acid, 80 ml water, 80 ml acetic acid and 200 ml ethanol. The samples were immersed in the solution for two seconds and then cooled with ethanol spray gun. After that, the samples were ready for microscopic investigations.

Qualitative metallography was conducted to measure the grain size of the samples. It was done as the following planimetry method by making the three subsequent circles on the optical micrograph then quantitatively measured the point of intersection. It was conducted at magnification of 20x within five times iteration. The total length of the circle line was 50 cm with ratio of 2 cm scale bar. The true line then measured to be 750 μm .

3.4. TENSILE TEST

The tensile samples have been prepared according to ASTM E8M with variation of nominal thickness and direction. The nominal thicknesses are 0.25, 0.5 and 1 mm with deviation of ± 0.05 mm. There were two directions observed for tensile testing: RT and TR, as shown in **Fig. 3.1**. The tensile samples were then marked on the gauge length as shown in **Fig. 3.3** in order to allow the non-contact video extensometer (NCX[®]) method.

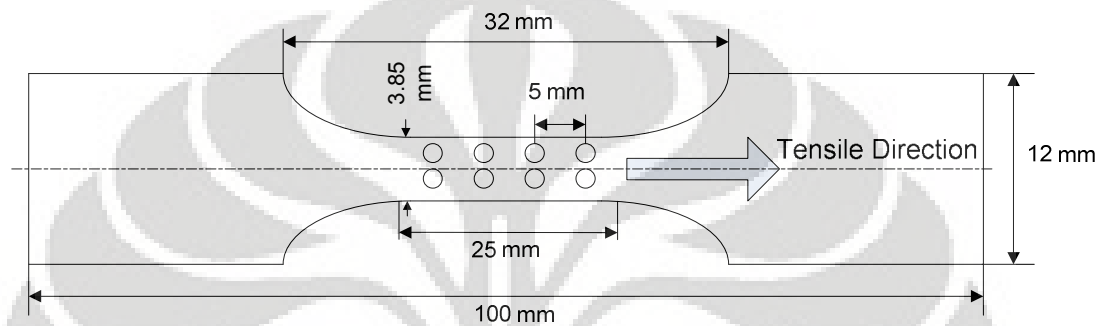


Figure 3.3 Schematic diagram of tensile specimen

The marks were made by using a 4-dot based device, specifically designed for tensile video extensometer. A multi-dot-based device required to mark the sample surface as shown in **Fig. 3.3**. This 4-dot-based system is a standard conventional for Mini Instron video extensometer. Initially, the sample surface was gently sprayed around the gauge length area to enhance accurate measurements on video camera. It is because tensile sample has rough and harsh surface for camera resolutions to capture particular marked on the surface. A very fine marker was used to give the identical dots on the surface. The tensile test was then conducted by using an INSTRON 5848 mini tester.

The Instron 5848 machine consists of two additional apparatus compare to conventional tensile machine. They are video camera and LED light. The video camera was calibrated before commencing the test. A software tool called NCX[®] was used for the accomplishment of the test.

Conventional tensile test was conducted on all samples with constant strain rate of 0.0005 mm/s. On the other hand, jump test was conducted with initial strain rate of 0.0005 mm/s which then slightly increased in an interval of $\sim 1.2 - 2$ % of strain. Before further increased, the strain rate was returned to 0.0005

mm/s for a certain interval of strain. The details of increment of strain rate can be seen in **Fig. 3.4**. The final strain rate in jump test was 0.005 mm/s. Strain rate sensitivity (m) was then calculated by using **Eq. 3.2** [1].

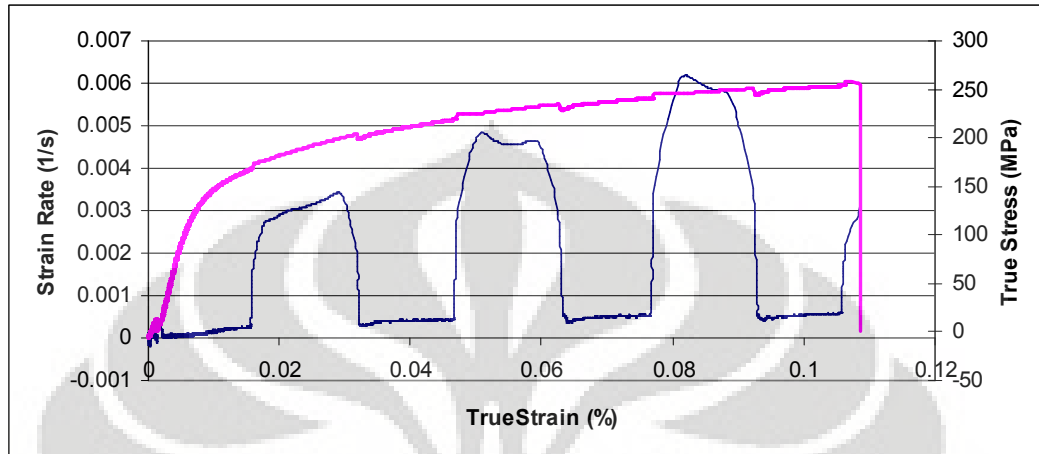


Figure 3.4. True Strain Vs Strain Rate

$$m = \left(\frac{\partial \ln \sigma}{\partial \ln \dot{\epsilon}} \right)_{\epsilon, T} = \frac{\dot{\epsilon}}{\sigma} \left(\frac{\partial \sigma}{\partial \dot{\epsilon}} \right)_{\epsilon, T} = \frac{\Delta \log \sigma}{\Delta \log \dot{\epsilon}} = \frac{\log \sigma_2 - \log \sigma_1}{\log \dot{\epsilon}_2 - \log \dot{\epsilon}_1} \quad (3.1)$$

$$m = \frac{\log (\sigma_2 / \sigma_1)}{\log (\dot{\epsilon}_2 / \dot{\epsilon}_1)} \quad \dots \dots \dots (3.2)$$

Both true stress-strain and engineering stress-strain data were given for each accomplishment of test. A further analysis on the tensile properties for each sample was calculated with Excel including yield strength, elastic modulus, ultimate tensile strength, total elongation and strain-rate-sensitivity respectively. In addition the images during the test can be obtained for every 2 seconds at one shoot. However, this data was not used in this project. Mechanical anisotropy (r) was also calculated by using the data on the distortion of dots on the sample, following the equation (3.3).

$$r = \frac{\epsilon_w}{\epsilon_t} = \frac{-\epsilon_w}{\epsilon_l + \epsilon_w} \quad \dots \dots \dots (3.3)$$

Fracture surfaces of conventional tensile test were observed macroscopically by using digital camera 7.2 MP. The detail of the non-contact video extensometer (NCX[®]) method with the use of MiniInstron Tensile Test machine is shown in **Fig. 3.5**.

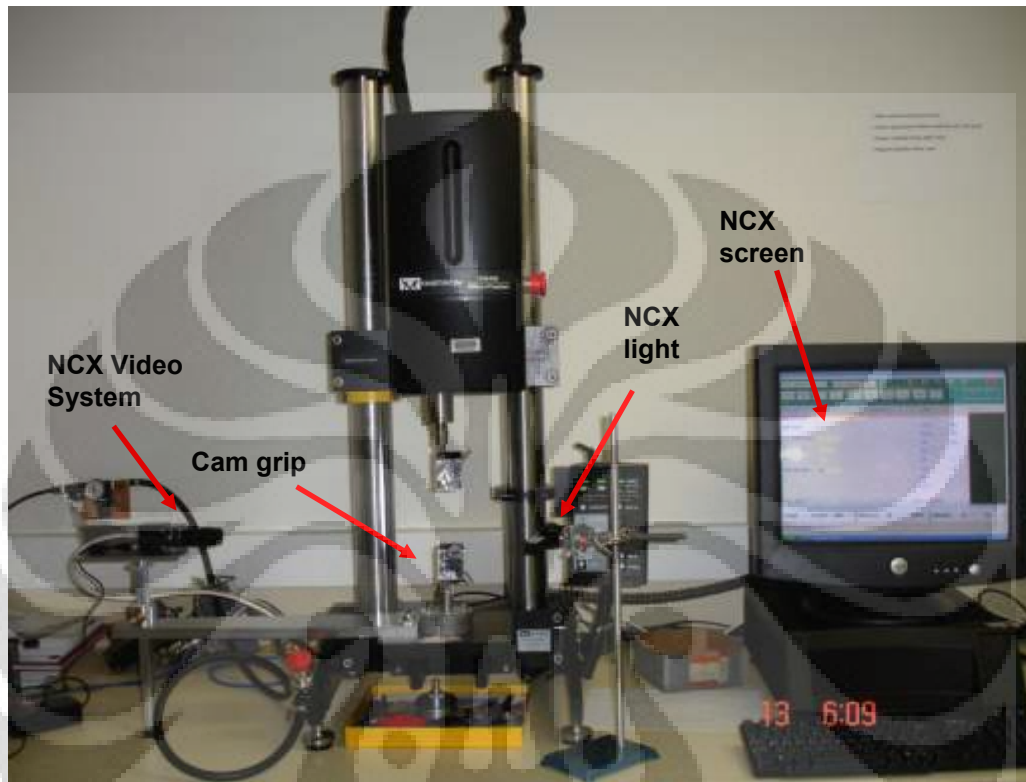


Figure 3.5. Model of MiniInstron 5848 with integrated major components

CHAPTER IV RESULTS AND DISCUSSION

4.1. TENSILE CHARACTERISTICS OF AZ31 MAGNESIUM ALLOY PLATE

Table 4.1, 4.2, 4.3, and **4.4** display the results of tensile test of AZ31 magnesium alloy plate by using conventional method for RT, TR NR, and TN direction, respectively. The characteristics that were observed from the test are 0.2% proof strength, ultimate tensile strength, total elongation, elastic modulus and anisotropy value (r). Each characteristic is tabulated for each single thickness.

In general, from **Table 4.1** and **4.2**, the 0.2% proof stress and ultimate tensile strength are generally higher at samples of TR direction than those of RT direction. The value of 0.2% proof strength ranges from 99 – 123 MPa for RT direction and 95 – 154 MPa for TR direction. The value of strength is confirmed to those in earlier studies [1]. According to the earlier studies, the tensile properties achieved in-situ tension shows the transverse (TR) direction has higher hardening rate during plastic deformation than that of longitudinal (RT) direction. It was matched with the experimental data for ultimate tensile strength ranges from 203 – 272 MPa for TR direction while 184 – 266 MPa for RT direction.

In addition **Table 4.2** and **4.4** are likely the same due to same plate direction that are TR and TN. The 0.2% proof stress shows 95 – 151 MPa for TR direction while another ranges from 140 – 151 MPa for TN direction. The total elongation, elastic modulus and anisotropy value are slightly different in average between TR and TN direction. In contrast, **Table 4.3** has significant result compare to other tabulated data. It is the NR direction with the lowest 0.2% proof stress that ranges from 64 – 85 MPa. It has ultimate tensile strength of 167 – 270 MPa with total elongation of 5.7 – 13.7 %. It is expected that high tensile strength then high elongation.

Effect of thickness on tensile properties generally increased as the thickness increased. The details of the thickness effect on the tensile properties can be seen on **Fig. 4.1, 4.2, 4.3,** and **4.4** together with the deviation for each point.

Table 4.1. Tensile test result of AZ31 Mg Alloy Plate at RT direction

Tensile Properties	Thickness [mm]		
	0.2	0.5	1
0.2% Proof Stress [MPa]	99 ± 30	118 ± 34	123 ± 35
Ultimate Tensile Strength [MPa]	184 ± 47	247 ± 54	266 ± 59
Total Elongation [%]	2.4 ± 0.74	8.3 ± 2.5	10.8 ± 3.4
Elastic Modulus (E) (GPa)	35 ± 1.1	24 ± 1.3	25 ± 0.3
Anisotropy value (r)	N/A	1.08666	1.328843

Table 4.2. Tensile test result of AZ31 Mg Alloy Plate at TR direction

Tensile Properties	Thickness [mm]		
	0.2	0.5	1
0.2% Proof Stress [MPa]	95 ± 28	169 ± 48	151 ± 43
Ultimate Tensile Strength [MPa]	203 ± 51	248 ± 55	272 ± 58
Total Elongation [%]	2.5 ± 0.75	7.9 ± 2.4	11.6 ± 3.7
Elastic Modulus (E) (GPa)	24 ± 2.8	26 ± 0.7	22 ± 2.1
Anisotropy value (r)	N/A	1.75987	1.72093

Table 4.3. Tensile test result of AZ31 Mg Alloy Plate at NR direction

Tensile Properties	Thickness [mm]		
	0.2	0.5	1
0.2% Proof Stress [MPa]	85 ± 16	64 ± 10	85 ± 7
Ultimate Tensile Strength [MPa]	167 ± 41	254 ± 35	270 ± 28
Total Elongation [%]	5.7 ± 2.7	11.2 ± 3.8	13.7 ± 2.4
Elastic Modulus (E) (GPa)	36 ± 5.4	19 ± 2	35 ± 3.5
Anisotropy value (r)	N/A	1.45697	1.62483

Table 4.4. Tensile test result of AZ31 Mg Alloy Plate at TN direction

Tensile Properties	Thickness [mm]		
	0.2	0.5	1
0.2% Proof Stress [MPa]	140 ± 11	149 ± 3	151 ± 12
Ultimate Tensile Strength [MPa]	192 ± 11	228 ± 15	239 ± 18
Total Elongation [%]	6 ± 1.5	9 ± 2.5	11 ± 3.8
Elastic Modulus (E) (GPa)	29 ± 3.5	26 ± 0.5	33 ± 5
Anisotropy value (r)	N/A	1.15087	1.81493

At all samples, the 0.2 mm thickness did not display due to material are not reliable to be tested. This comes from the easiness of material to be bent during the setting up of the tensile machine. Another experimental error was considered which is shown from the huge deviation of each property. It was caused from the light sensitivity of the video camera and also the irregularity of

the grips. The pneumatic grips did not tighten enough to bite the thinnest sample. Therefore, the 0.2 mm samples experienced low reliability and hence no assurance data for r -value.

According to **Eq. 3.3** ε_l , ε_w , and ε_t are the logarithmic strains along the length, width, and thickness directions, respectively. Important parameters affecting plastic instabilities are the strain hardening rate (n) and strain-rate-sensitivity (m). The results given that transverse (TR) direction has higher anisotropy value of 1.73 compared to longitudinal (RT) one with 1.32. With higher anisotropy value the ability of material to be shape with only a slight change in thickness, especially, deep drawing is easier [2]. However, strong variations in anisotropy value within the sheet plane (e.g planar anisotropy) can cause forming problems such as earing [6]. The corresponding anisotropy on this project was observed at $\sim 7\%$ plastic strain similar to what literature stated by which the maximum tensile strain that twinning may accommodate is only at 0.065 strain or equal with 6.5% [2]. This argument experimentally proved when strain ranges at 6 – 7 %, there was a “twinning voice” generated from tensile sample.

4.1.1. Elastic Modulus

The elastic modulus for each plate orientation is shown in **Figure 4.1**. It is clearly seen that the value of the elastic modulus ranging from 19 – 36 GPa. Among the four plate orientations, in average the NR samples possess the highest and the lowest value of elastic modulus, though peculiar result occurred at 0.5 mm thick sample. Based on elastic modulus ranges, the results are approximately half of the literature data [9]. Error bar is shown for each data point calculation. It can be seen the NR sample direction has the largest error bar at 0.2 mm sample thickness.

In terms of effect of thickness, the TR and TN sample directions are generally constant while the NR and RT are slightly decreased followed by gradual incline as the thickness increased. In addition to effect of direction, the four plate direction can be categorized into three general categories TR, RT, and NR. Those TR and TN direction have same rules.

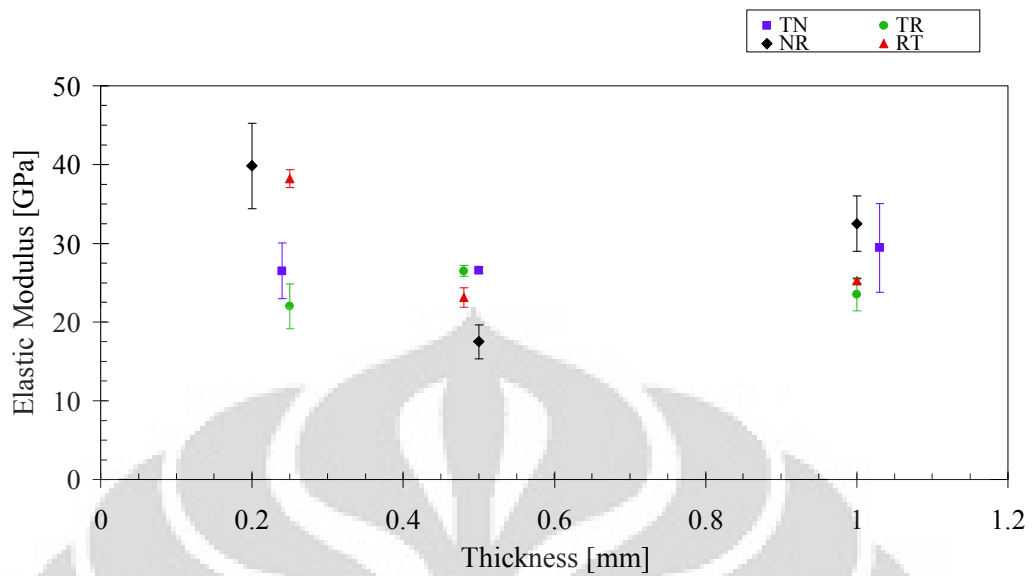


Figure 4.1 Elastic modulus of magnesium alloy plate AZ31 at different tensile directions

The main reason behind of the half elastic modulus value is coming from the phenomenon of microyielding. Microyielding accommodate the slip deformation which probably occurred during the elastic region. As it mentioned above, the 0.2 mm samples are not reliable to represent the characteristic of tensile properties.

4.1.2. Ultimate Tensile Strength (UTS)

The ultimate tensile strength for each plate orientation is displayed in **Figure 4.2**. In general, the ranges of the value of ultimate tensile strength are 142 – 270 MPa. The highest tensile strength possessed by NR sample direction while the lowest one is RT sample direction. According to literature data, for hot-rolled product the ultimate tensile strength is 220 MPa while the extruded product is ~ 290 MPa [1]. The middle ranges of the experimental data is still fulfilled the literature data.

The trends of each sample direction are increases as the thickness increases. Though between 0.5 and 1 mm thick, the values are slightly increased and some of them experienced level-off. In terms of plate orientation, the NR sample direction still posses the highest position while RT sample direction takes place at the lowest one. It is contrast with elastic modulus chart at which the trend

of the NR sample direction is decreased. It is due to the easy slip deformation and tensile twin to be activated in sample with uniaxial tensile direction parallel to basal plane.

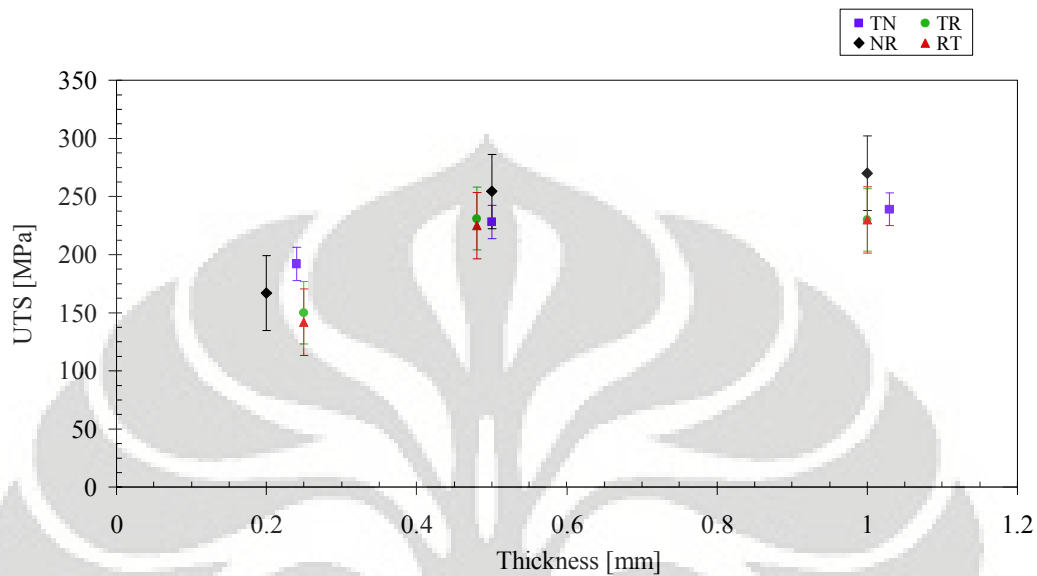


Figure 4.2 Ultimate Tensile Strength of magnesium alloy plate AZ31 at different tensile directions

4.1.3. 0.2 % Proof Stress

The relationship between 0.2% proof stress and different tensile direction are described in **Figure 4.3**. In general, the ranges of the experimental data are 64 – 163 MPa. Proof stress is simply defined the stress required to produce a very slight specified amount of plastic strain [10]. In this case, the lower position possessed by NR sample direction and the highest owned by RT one. It is opposite with ultimate tensile strength chart by which NR sample direction possess the highest value. The true stress-strain curve generated from NR sample direction has shallow elastic region with a very huge plastic region. Once the plastic strain initiated, deformation mechanism takes place the whole process. Either sample experienced dislocations slip or mechanical twins as the response for the deformation load. Since the test was conducted at room temperature then probability for both mechanism to occur are then taking into account.

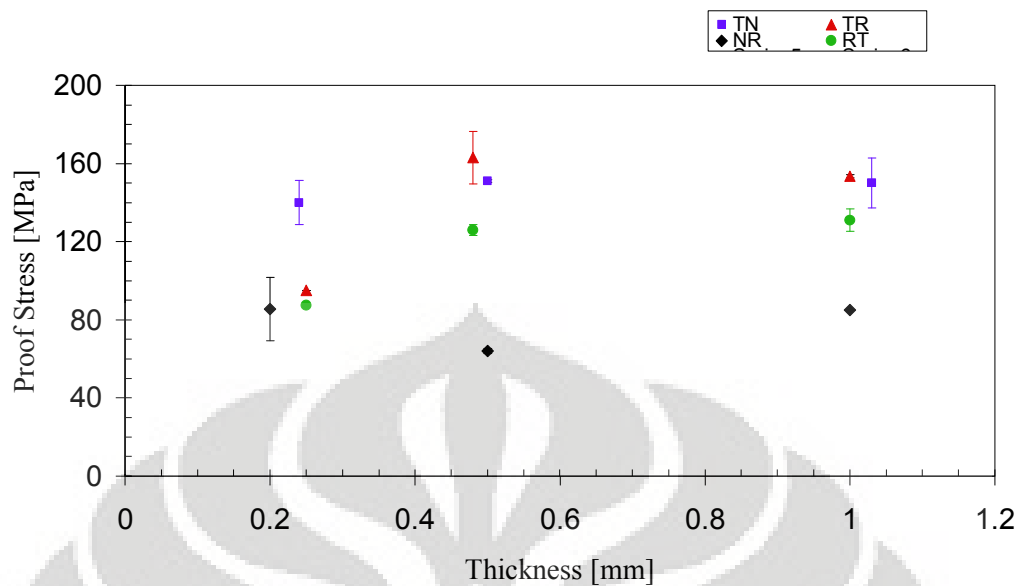


Figure 4.3 Proof Stress of magnesium alloy plate AZ31 at different tensile directions

In terms of effect of thickness, all three samples direction that are TR, TN, and RT have general trend increases. Meanwhile the NR sample has general trend decreases and then gradually increases. The easy deformation slip plane which is in this case owned by NR specimen has influenced by the number of grains which believed accommodate the critical resolved shear stress (CRSS) to occur. Either the specimen is classified as to have fine grains or coarse grains; the thickness effect against the mechanical properties is strongly dependent on the structure of the grains.

4.1.4. Elongation-to-failure (EL)

The total elongation for each sample direction is described in **Figure 4.4**. It can be seen that the ranges of the total elongation are between 3.6 – 13.7 %. The lowest elongation belongs to RT sample direction while the highest one possessed by NR sample direction. The general trend shows that sudden increment occurred from 0.2 mm to 0.5 mm thick samples. It can be seen from the double increment of elongation. It is strongly related with the workability of material. Furthermore, NR sample direction was tested with c-axis parallel to the tensile direction which resulted in higher elongation than that of the three directions.

In terms of plate direction, all the samples show same rules. They are all increased. In addition to error bar, NR sample direction has larger error bar. It can be seen obviously the thickness effect on different plate orientations. At this stage, the thinnest thickness has considerably lower total elongation. It is almost doubled from the 0.5mm thickness. A very good explanation to this might due to the larger ratio in thickness over average grain diameter (t/d) aspect ratio [11].

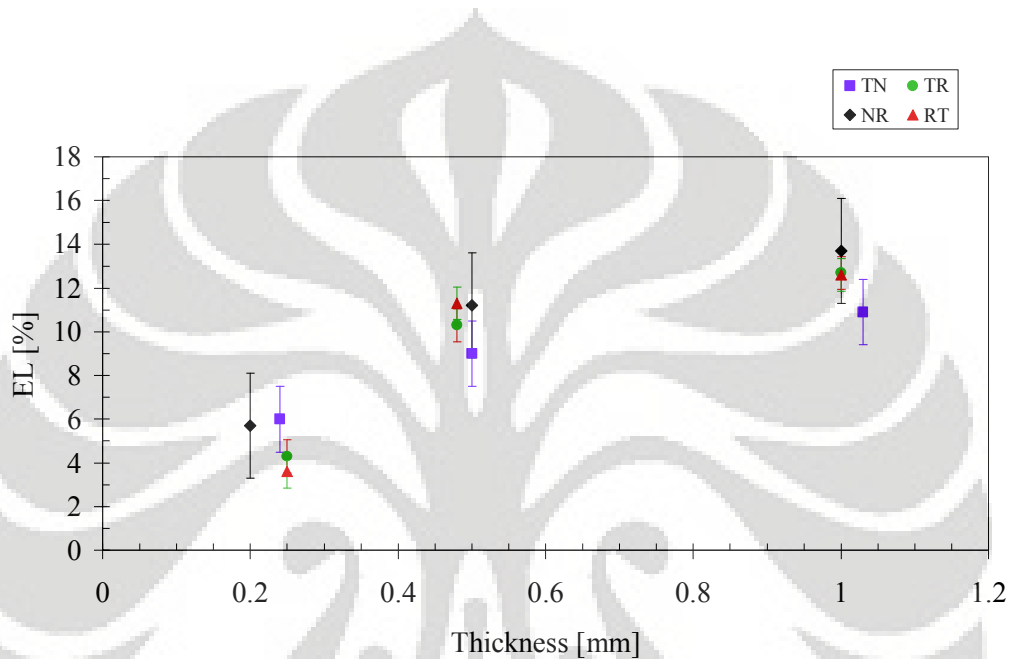


Figure 4.4 Total Elongation of magnesium alloy plate AZ31 at different tensile directions

In addition the ultimate tensile strength (UTS) has general trend the same with total elongation. At this stage, crystallographic structure plays important role in determining the tensile behaviour of corresponding specimens. Limited deformation mechanism applied for hexagonal metal structure. Therefore, strong correlation between texture figures followed by the sample orientation could explain the deformation history of each specimen. Furthermore the strain-rate-sensitivity (m) shows two different results. Again, plate orientation classified these discrepancy values. The NR specimen which tested along the c -axis produced an incline in work-hardening-rate while the others orientation TR, TN and RT have decline trends. Activation of non-basal slip might be the reason of low hardening rate and hence strain-rate-sensitivity [9]. Furthermore there was no

coherency between nominal and actual strain rate. It is because nonlinear curve on the true stress-strain which resulted in very high deviations from each data points.

4.1.5. Strain-Rate-Sensitivity

Among the four sample orientations only NR sample shows significance trend. It has negative value at lower strain and dramatically increases after the second point of strain. In the contrast, the other three samples have similar trends which have been indicated from their descendant trend over the larger true strain. Ideally such a work hardening rate occurred in NR trends indicated from incline trend of strain-rate-sensitivity whereas the work hardening might be less contributed for the sample orientation by which basal slip $\langle c \rangle$ was not parallel with the applied load [2].

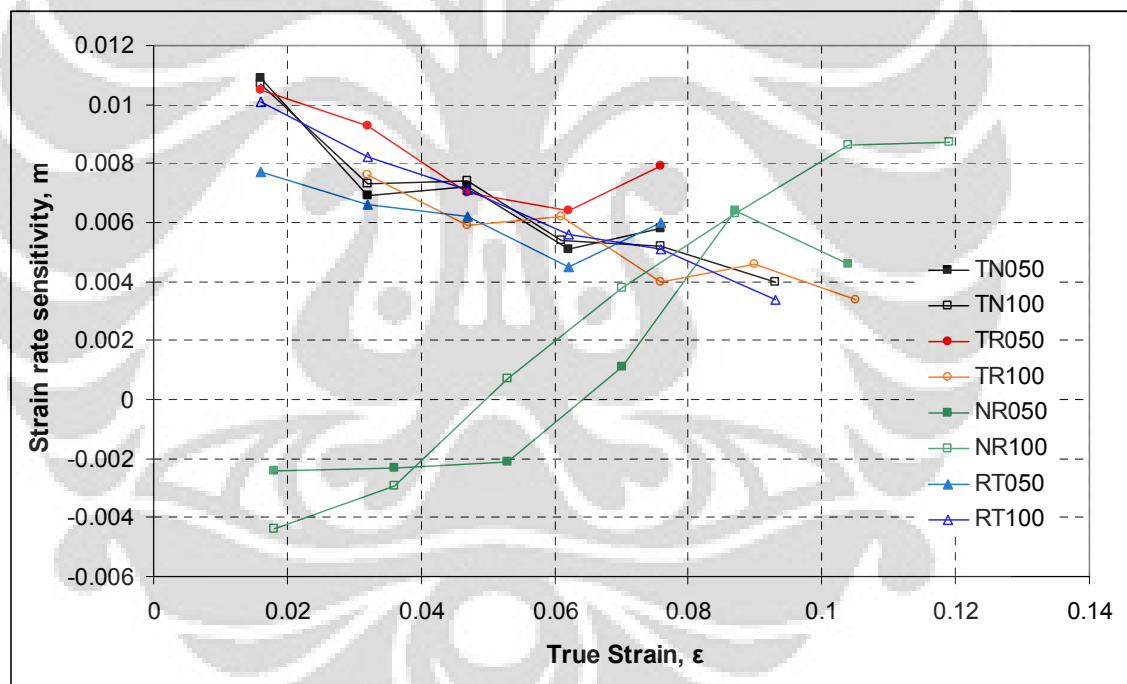


Figure 4.5 Strain rate sensitivity of magnesium alloy plate AZ31 at different tensile directions

In polycrystalline magnesium with a strong fibre texture tested at room temperature such an increase in strain rate leads to a moderate increase in tensile yield stress [12]. This statement can be explained from the plot of the true stress-strain curve. To this end, material with high elongation will have high increase in yield stress. It goes with the statement of strain-rate-sensitivity. A high increment shows good formability and hence better performance for further formability such as deep-drawing. It is really important because the process of metal-shaped magnesium alloys which takes place at room temperature have better properties for the applications due to fine-grained microstructure with no liquations or pores [6]. Furthermore cost product and aesthetic aspect of cold working were also behind this reason.

It has been subjected the occurrence of microyielding responsible for the lowering value of experimental result. The reason behind this is because the curve of stress-strain was linear resulting in very large ranges of data interval used to calculate the slope. When the slope being projected into a curve, a huge elastic deviations revealed. However, recent published paper pointed out that solid material which has high c/a ratio or a complex unit cell with a large a -lattice parameter was classified as kinking nonlinear elastic (KNE) [9]. Thus hexagonal metals particularly magnesium is plastically anisotropic and in order to allow plastic deformation occurs, a very complex deformation systems undertake the place. In this case, authors explained in between threshold stress (σ_t) and yield point (σ_y), the phenomenon of microyielding takes place [9]. Furthermore, the previous work was analyzed the nonlinear response is due to the formation of incipient kinking bands (IKBs) on the easy slip system, namely basal plane. At all, it also pointed out if the IKBs associated with σ_t and W_d are strong functions of grain size, with larger grains resulting in lower σ_t but higher W_d and vice versa.

4.2. MICROSTRUCTURE OBSERVATION

In order to obtain adequate information in regard with images, two subsequent experimental images were conducted. Those are optical micrograph and general images. The optical micrograph compromise with before and after

deformation by which as-received images represent the three nominated sample directions. The macro-images were then taken with 7.2 camera digital.

4.2.1. Optical Micrograph

The grains size measurement for as-received material was conducted with planimetry method with length of true line 750 μm and magnification 20X. It shows homogenous grains distribution with equiaxed grains. In addition, the average grain sizes of as-received specimens were about $26.5 \pm 5 \mu\text{m}$. It is convenience because the plate was hot-rolled and such a recrystallization took place during hot working. Furthermore, the ratio of tensile twinning in NR sample was found much higher than the others sample. Again, it is caused by the deformation modes which parallel with the c-axis and hence the activation of such a mechanical twinning is much easier compare to other specimens which need larger stress to activate non-basal plane [1, 2].

4.2.1.1. As-received

All three surface images were examined towards the direction of sample sectioning as it shown in **Fig. 4.6a**. Grain size was measured by using planimetry method and the results were then taking into account as shown in **Table 4.5**. Generally, homogeneous microstructure will produce for hot-rolled product since dynamic recrystallization (DRX) takes place during the deformation. Though some interior grains have larger grains it might be caused by which the observed surface was polished not parallel to the sample plane.

Table 4.5 Average Grains Size of specimen as-received

Face Direction	Average Grains Size (μm)
RT-TD	25.17 ± 3.7
TD-ND	24.04 ± 1.6
ND-RD	26.59 ± 5.1

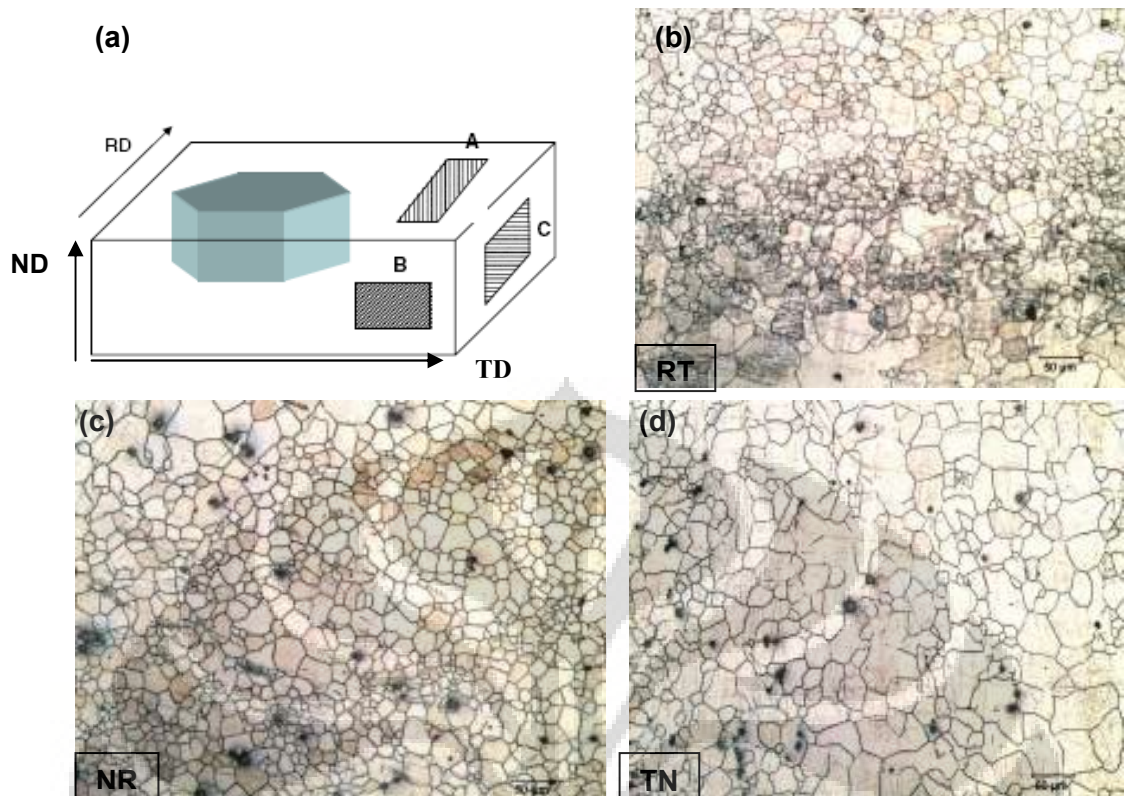


Figure 4.6 Microstructure of as-received specimen directional relative to rolling direction. Taken from (a) longitudinal plane, (c) normal plane, (d) transverse plane

4.2.1.2. *As-deformed*

The microstructure of magnesium deformed by tensile test is shown in **Figure 4.7**. They are all content tensile twins distributed uniformly throughout the images. The tensile direction is on the right hand side and the surfaces examined were taken from lateral side (sample thickness). In the case of NR sample, the amount of tensile twins is much higher than the others followed by numbers of uniform fine grains. In contrast, the appearance of tensile twins in other three samples was located mainly at the exterior grains and comprises of mix coarse and fine grains.

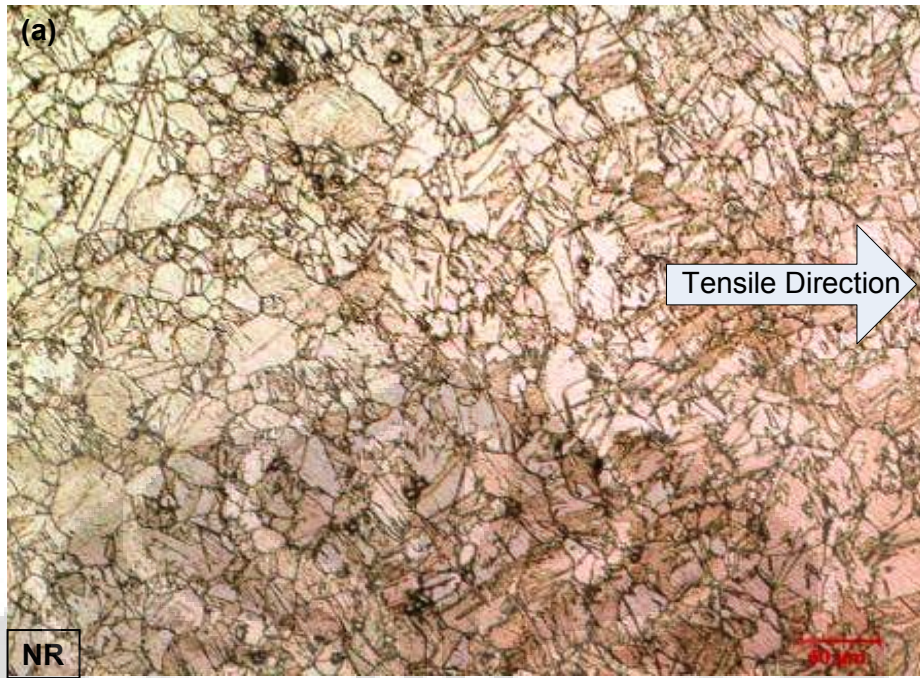


Figure 4.7 (a) Microstructure of specimen deformed by tensile test, $\epsilon = 13.7\%$.

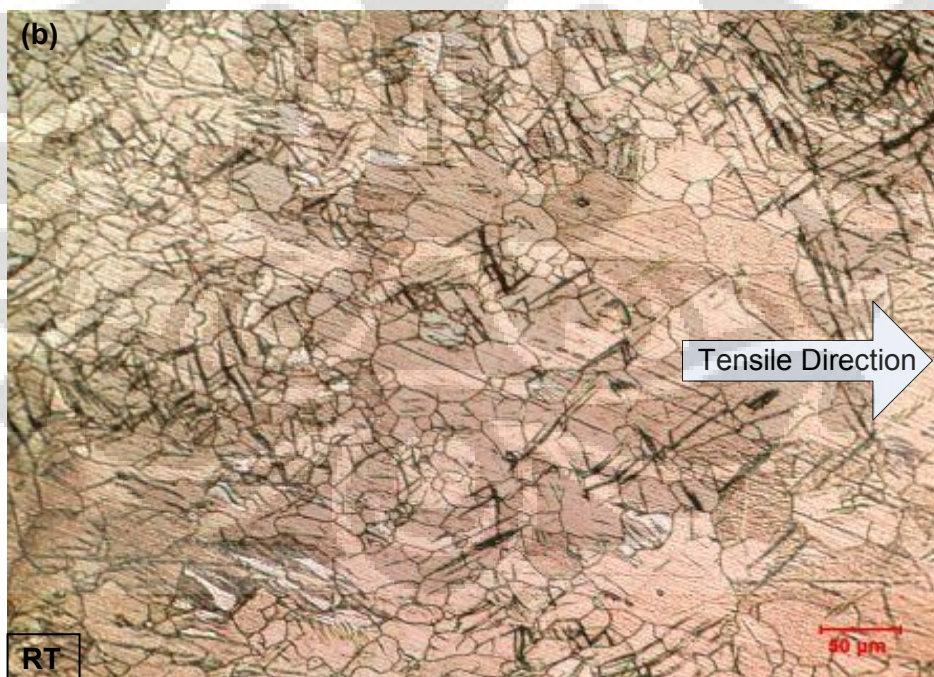


Figure 4.7 (b) Microstructure of specimen deformed by tensile test, $\epsilon = 12.6\%$.

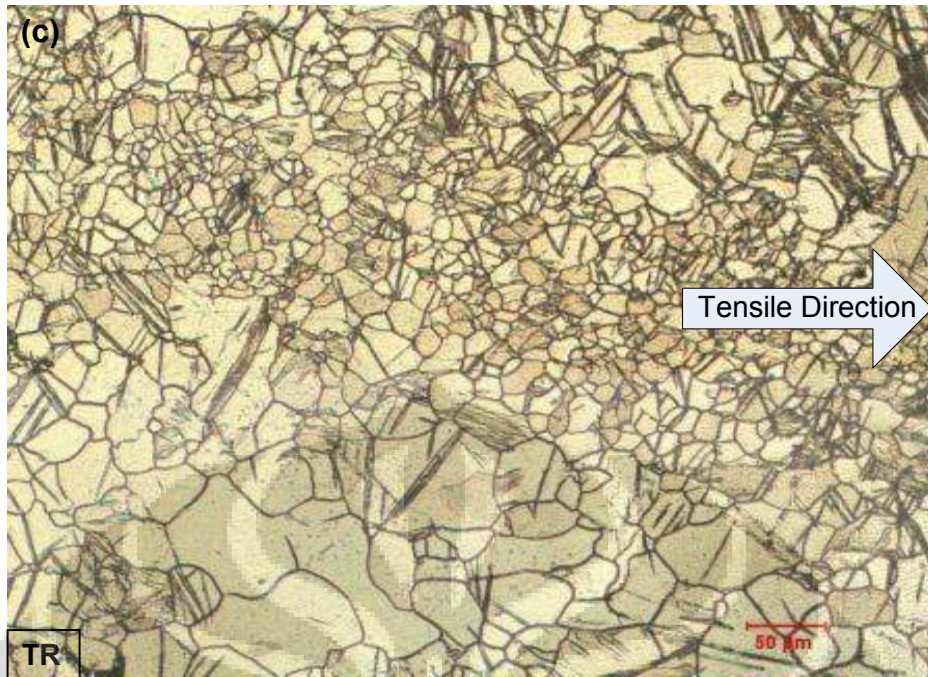


Figure 4.7 continued (c) Microstructure of specimen deformed by tensile test, $\epsilon = 10.9$ %.

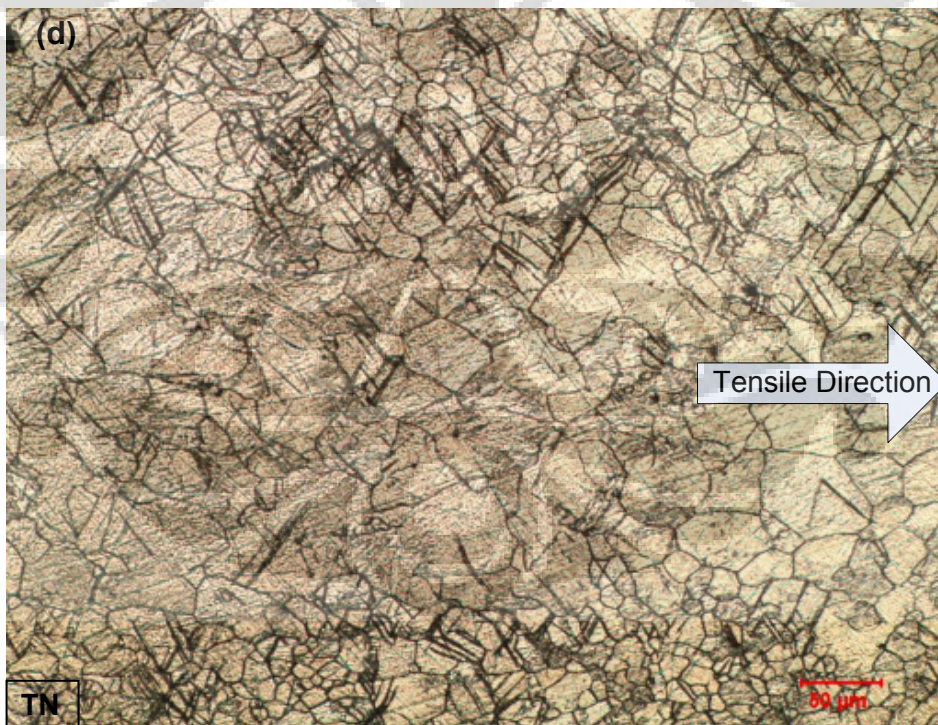


Figure 4.7 continued (d) Microstructure of specimen deformed by tensile test, $\epsilon = 12.7$ %.

It has been mentioned before that to activate the corresponding basal $\langle c \rangle$ plane at higher temperature is quite easy since it has low critical resolved shear stress (CRSS) [1]. But it is not the case for the significant occurrence to explain the TN sample has fracture like peak sharp fracture just like a tip of knife. Apart from deformation slips mechanism, tensile twinning on $\langle 10\text{-}12 \rangle$ is subjected for the mechanical behaviour in of polycrystalline plastic deformation [7]. Based on other investigators *Yoshinaga* and *Horiuchi* in 1963 pointed out some twinning mechanism was observed to barely precede fracture. Having thus statement in mind then it can be deduced that such a heavy mechanical twinning took place in NR sample. Further explanation to this is because most of them have an early fracture occurred before it broken at the gauge length. Yet, the sample itself was also slightly moved (against from each other) once the early indication of fracture propagated. This can be further explained that twinning is a polar mechanism that only allowing simple shear in one direction, rather than both forward and backward directions like dislocation slip [2].

4.3. MACROSCOPIC IMAGES

The macroscopic features were taken for each samples orientation. It was taken for all 1mm samples thick. Three out of four specimens show brittle fracture whilst another one experienced ductile-to-brittle fractures. It was the TN sample which shows this peculiarity by which such a peak sharp fracture area is shown in **Figure 4.8**. Further to this phenomenon, it is believed that tensile twinning underwent through the specimen orientation. The activation of non-basal plane might be responsible for the occurrence of this feature. The detailed of the explanation will be discussed in the following sections.

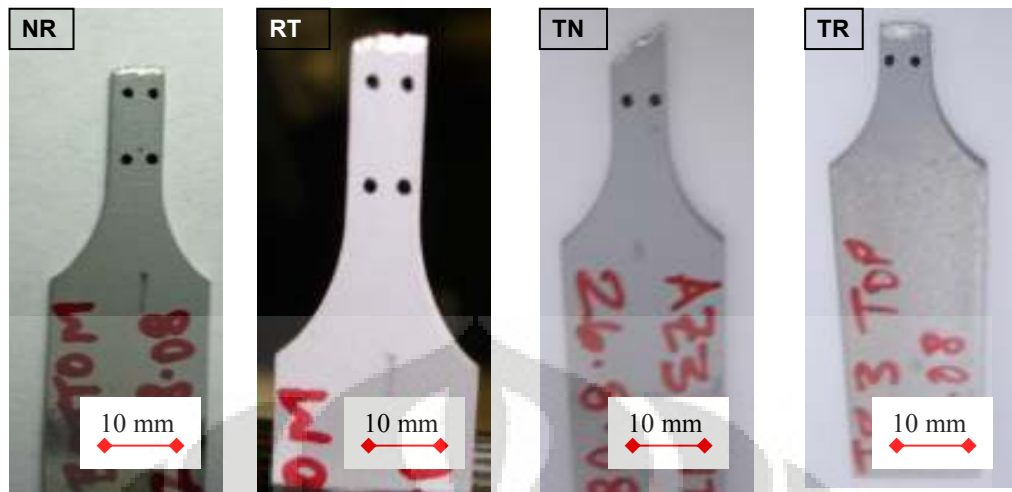


Figure 4.8. Macroscopic features of specimen deformed by tensile test, taken by 7.2 MP digital camera

There are literature journals reported that the formability of magnesium at room temperature is much more complex than at elevated temperatures [2,9]. The history of material is; however, plays important role in providing relevance information for further samples interrogation. This aspect covers the information on materials processing, chemical composition, and texture figures. There is strong relationship of deformation modes on the initial textures and therefore forming process. The effects observed indicating that primary basal $\langle a \rangle$ slip in hexagonal metal is predominantly activated along with tensile twinning conducted at ambient temperature. The effect is even more marked when Von misses criterion applied to conform the 5 independent slip systems in correspond to energy of shear deformation in Critical resolved shear stress (CRSS) [1,2].

CHAPTER V

CONCLUSION AND FUTURE WORK

The results of the projects can be compiled into some points as the following:

- The increase of sample thickness from 0.2 to 1 mm increases the proof stress for 20%, 37%, 24% and 0.8% for RT, TR, NR, and TN directions, respectively.
- The increase of sample thickness from 0.2 to 1 mm increases the ultimate tensile strength for 31%, 25%, 38%, and 20% for RT, TR, NR and TN directions, respectively.
- The increase of sample thickness from 0.2 to 1 mm increases the total elongation for 77%, 78%, 58%, and 45% for RT, TR, NR, and TN directions, respectively.
- There were no effect of thickness were observed on elastic modulus.
- Samples with NR direction showed more twinning, indicating more deformation occurred than that of other samples direction.
- There is an effect of plate direction on tensile properties particularly on NR sample direction which has tensile direction parallel with the c-axis.
- The strain rate sensitivity for all three samples direction TN, TR, and RT were gradually decreased as the true strain increased while the NR sample direction has inclination trend.
- In average, the grain size was the same before the tensile test with averages of 25 μm and appeared with more heterogeneous grains.

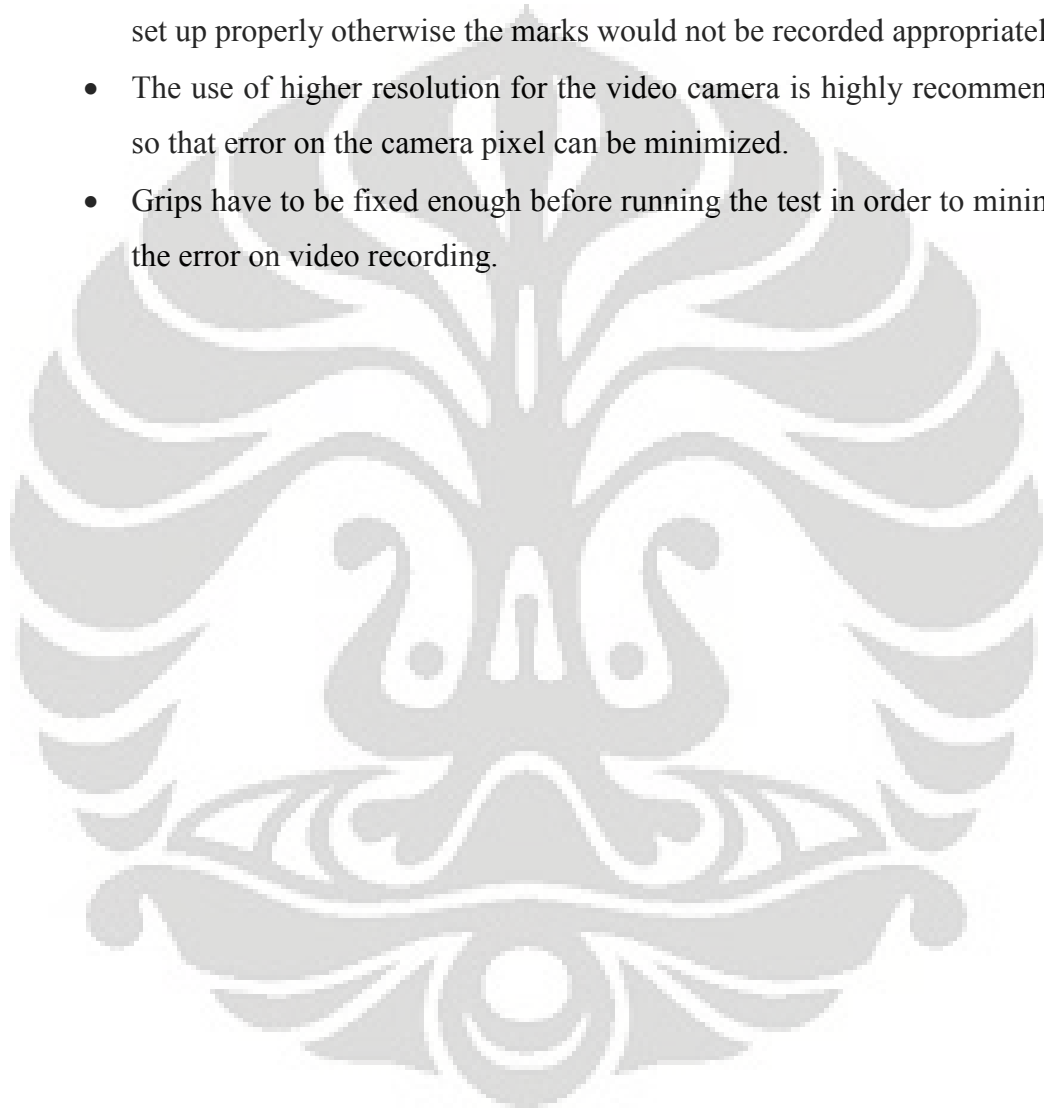
Based on the work done so far there are three areas evident as suitable direction for future work. Those three areas are:

- In-situ texture measurements by which initial texture as well as texture evolution as the response on the activation of deformation systems during the test can be investigated during the whole deformation process.
- Conducting the interrupted test method to study the effect of work hardening rate subjected for workability of particular sheet Mg products.

- Texture simulation based on a particular implementation of the viscoplastic self-consistent (VPSC) model. This model allows heterogeneity of each crystallite so that the anisotropic behavior observed in hexagonal is well described.

Suggestion can be given for further work as the following:

- Lighting for the non-contact video extensometer (NCX[®]) method has to be set up properly otherwise the marks would not be recorded appropriately.
- The use of higher resolution for the video camera is highly recommended so that error on the camera pixel can be minimized.
- Grips have to be fixed enough before running the test in order to minimize the error on video recording.



REFERENCES

- [1] Yi, Sangbong., *Investigation on Deformation Behaviour and the Texture Evolution in Magnesium Wrought Alloy AZ31*. Dissertation Paper, 2005. University of Clausthal.
- [2] S.R. Agnew, O. Duygulu: *Int. J. Plasticity.*, vol. 21 (2005), pp 1161-1193.
- [3] M.R. Barnett: *Metall. And Mater. Trans.*, vol. 34A (2003), pp 1799-1806.
- [4] Rosenbaum H.S. (1964), *Nonbasal slip in hcp metals and its relation to mechanical twinning*, *Deformation Twinning*: ed. Reed-Hill R.E, Hirth J.P., Rogers H.C., Gordon and Breach, NewYork.
- [5] Koike. J, Kobayashi.T: *Act Mat.*, vol. 51 (2004), pp 2055-2065.
- [6] Kainer, K.U., *Magnesium Alloys and Technology*, Willey-VCH, 2003, page. 79.
- [7] Gottstein. G, T. Al Samman: *Mat. Sci. Forum.*, vol. 495-497 (2005), pp 623-632.
- [8] S. Graff, B. Wolfgang, Steglich, D: *Int. J. Plasticity.*, vol. 23 (2007), pp 1957-1978.
- [9] S.V.S. Narayana Murty et all, *Development of High Strength Bulk Ultrafine-Grained Magnesium Alloy AZ31 by Mulit-Pass Warm Rolling*. Proceedings of the International Conference on Aerospace Science and Technology, June 2008, Bangalore, India
- [10] A.G. Zhou, S. Basu, M.W. Barsoum: *Acta Materialia.*, vol. 56 (2008), pp 60-67.
- [11] A. Molotnikov, R. Lapovok, C.H.J. Davies, W. Caoa, Y. Estrin: *Scripta Mater.*, vol. 59 (2008), pp 1182-1185.
- [12] William D. Calister, *Materials Science and Engineering An Introduction*, 6th Edition, 2004, Willey.
- [13] C.H.J Davies: *Mat. Sci. Forum*, vol. 539-543 (2007) pp. 1723-1728

APPENDIX

Strain-rate-sensitivity of the accelerated deformed testing

TN	True Strain	$\epsilon = 0.016$	$\epsilon = 0.032$	$\epsilon = 0.047$	$\epsilon = 0.062$	$\epsilon = 0.076$	$\epsilon = 0.093$	
TN050	SRS	0.0109	0.0069	0.0072	0.0051	0.0058		
TN100	SRS	0.0107	0.0073	0.0074	0.0054	0.0052	0.0040	
NR	True Strain	$\epsilon = 0.018$	$\epsilon = 0.036$	$\epsilon = 0.053$	$\epsilon = 0.070$	$\epsilon = 0.087$	$\epsilon = 0.104$	$\epsilon = 0.119$
NR050	SRS	-0.0024	-0.0023	-0.0021	0.0011	0.0064	0.0046	
NR100	SRS	-0.0044	-0.0029	0.0007	0.0038	0.0063	0.0086	0.0087
TR	True Strain	$\epsilon = 0.016$	$\epsilon = 0.032$	$\epsilon = 0.047$	$\epsilon = 0.062$	$\epsilon = 0.076$	$\epsilon = 0.090$	$\epsilon = 0.105$
TR050	SRS	0.0105	0.00093	0.0070	0.0064	0.0079		
TR100	SRS	N.A	0.0076	0.0059	0.0062	0.0040	0.0046	0.0034
RT	True Strain	$\epsilon = 0.016$	$\epsilon = 0.032$	$\epsilon = 0.047$	$\epsilon = 0.062$	$\epsilon = 0.076$	$\epsilon = 0.093$	
RT050	SRS	0.0077	0.0066	0.0062	0.0045	0.0060		
RT100	SRS	0.0101	0.0082	0.0071	0.0056	0.0051	0.0034	

